J. Chem. Sci. Vol. 128, No. 1, January 2016, pp. 153–158. © Indian Academy of Sciences.
DOI 10.1007/s12039-015-1006-8

Anodization of Aluminium using a fast two-step process

MURUGAIYA SRIDAR ILANGO, AMRUTA MUTALIKDESAI and SHEELA K RAMASESHA*
Divecha Centre for Climate Change, Indian Institute of Science, Bangalore 560 012, India
e-mail: sheela@caos.iisc.ernet.in

MS received 10 August 2015; revised 26 October 2015; accepted 10 November 2015

Abstract. Ultra-fast two-step anodization method is developed for obtaining ordered nano-pores on aluminium (Al) foil. First anodization was carried out for 10 min, followed by 3 min of second anodization at high voltage (150 V) compared to previous reports of anodization times of 12 h (40-60 V). The pore dimensions on anodized alumina are 180 nm for pore diameter and 130 nm for inter-pore distance. It was evident that by increasing the anodization voltage to 150 V, the diameter of the pores formed was above 150 nm. The electrolyte and its temperature affect the shape and size of the pore formation. At lower anodization temperature, controlled pore formation was observed. The anodized samples were characterized using the field emission scanning electron microscope (FE-SEM) to determine the pore diameter and inter-pore distance. Using UV-Visible spectroscopy, the reflectance spectra of anodized samples were measured. The alumina (Al_2O_3) peaks were identified by x-ray diffraction (XRD) technique. The x-ray photo electron spectroscopy (XPS) analysis confirmed the Al 2p peak at 73.1 eV along with the oxygen O 1s at 530.9 eV and carbon traces C 1s at 283.6 eV.

Keywords. Anodization; phosphoric acid; anodization time; anodized aluminium oxide; aluminium.

1. Introduction

Anodization is the process of creating nanopores, on the surface of aluminium (Al) to form an anodic alumin ium oxide (AAO), using the method of electrochemical fabrication.[1,2] Anodization parameters control the arrangement of nanopore formation. The pores formed are parallel to each other and perpendicular to the surface of the foil.[3,4] The hexagonal structures in AAO are dependent on the type and concentration of the electrolyte, temperature, applied voltage and duration of anodization.[5–7] The AAO layer has a large band gap, good dielectric constant, mechanical strength and corrosion resistance.[8–11]

AAO templates are obtained using electrolytes such as oxalic, chromic, phosphoric or sulphuric acid.[12–16] The anodization voltage can be varied according to the type of electrolyte used. Sulphuric acid 0.3 M (25 V), phosphoric acid 0.1 M (150-195 V) and oxalic acid 0.3 M (40 V) for 12 hours of anodization time can form 63, 500 and 100 nm interpore distance respectively.[17–20] Organic electrolytes such as malonic and tartaric acid are also used to form self-ordered porous alumina films.[21] The temperature variations in the electrolyte affect the porosity of the anodized sample. The rate of formation of pores increases with increase in temperature.[22]

Different methods of anodization are single step, pre-patterned and two-step anodization. Single step anodization is carried out using sulphuric, oxalic and phosphoric acid to obtain nanoporic oxide layer which has non-uniform pores and inter-pore distance.[23] Pre-patterned anodization is a process of inscribing the patterns on the Al surface using techniques such as UV exposure, e-beam lithography. Later, anodization is carried out using oxalic acid to grow AAO templates.[24] Two-step anodization recently resulted in uniform self-organised nanopores on Al substrates. In two-step anodization, homogeneous or heterogeneous electrolytes are used to anodize the sample separately. Typically the first anodization takes a longer period (12 h at 195 V) for template formation;[25] this template acts as the pattern for the second anodization. In one of the reports, sulphuric acid was used as the electrolyte for the first anodization to form pits on Al substrate, while in second anodization these pits act as the pattern for nanopore formation.[26] Nanoporous alumina is used in the development of thermoelectric devices using metamaterials and for energy harvesting. Anodized magnetic nanohole arrays are used in biological and biomedical applications.[27]

In this paper, we report an anodization process where the total anodization time has been reduced from 12 h at 195 V[25] of previous reports to 15 min at 150 V and the self-ordering of the pores formed are in good

*For correspondence

agreement with the literature. The effects of anodizing parameters on the nano-pore formation are analysed. Two-step anodization process is followed to fabricate AAO templates with 180 nm pore diameter. The combination of oxalic acid in first anodization and phosphoric acid in second anodization is chosen with optimized anodization parameters for uniform pore formation.

2. Experimental

A high purity aluminium foil of 0.5 mm thickness (Merck-99.99%) was cut into strips of dimension 10 x 30 mm^2. These strips were ultrasonicated in de-ionized water and acetone for 5 min in each solution. The strips of Al were blow dried, annealed at 300°C for 10 min in the air ambient. The annealed samples were degreased using acetone and de-ionised water for 10 min separately. After degreasing, the sample was etched using 0.75 M sodium hydroxide by dipping the samples in the solution for 4 min. To reduce the surface irregularities, the samples were electro-polished in the solution containing 1:4 v/v mixture of perchloric acid ($HClO_4$) and ethanol (C_2H_5OH) at 7°C with a constant voltage of 15 V for 3 min. After electro-polishing, the Al strips were washed with de-ionized water and acetone. The porous AAO layer was fabricated by the two-step anodization process.

In the first step of anodization, oxalic acid was used as an electrolyte where the weak spots (pattern) were formed. The ultra-fast second anodization was carried out using orthophosphoric acid (H_3PO_4) electrolyte. In a hundred millilitre beaker, 80 mL of 0.3 M oxalic acid was prepared and carefully placed in polystyrene container filled with a mixture of grated ice and rock salt. The purpose of rock salt with the ice is to maintain the temperature below 273 K. By using a thermometer the temperature of the electrolyte was constantly verified. When the temperature of the solution reaches 280 K, the platinum coil which acts as the cathode was dipped in to the solution. Simultaneously, the electro-polished Al strip connected to the anode of DC power supply was inserted. Anodization was carried out for 10 min at a constant voltage of 40 V. Then the sample was rinsed in de-ionized water and dipped in an etching mixture of 3.5 wt% H_3PO_4 and 4.5 wt% of chromic acid (H_2CrO_4) at 353 K for 5 min. The above step removed the oxide layer formed during first anodization, leaving behind the weak point for the second anodization. The second anodization was carried out with a similar apparatus setup and 1% H_3PO_4 was used as the electrolyte at a constant voltage of 150 V at a temperature of 283 K for 2 min.

Pores in anodic aluminium oxide layer were characterized and analysed using FE-SEM images (Ultra 55, field emission scanning electron microscope (Carl Zeiss)). Physical properties such as pore diameter and interpore distance were measured and averaged considering the pores present in the FE-SEM images. The interconnected, incomplete pores were not taken into account. Reflectance spectra were taken from UV-Visible spectrometer (analytic jena SPECORD S-600) for analysing the differences between the absorption of anodized samples with different pore size. XPS (ultra AXIS) analysed the intensity peaks and orbital values. XRD (Bruker D8 advance) was used to identify the peaks of alumina after anodization.

3. Results and Discussion

Anodization process takes place with the oxygen ions present in the electrolyte which reacts with the surface of the Al to remove the Al^{3+} ions. The motivation of this work is to lower the time taken for the anodization process and to analyse the AAO pore formation using different acids such as oxalic and phosphoric acid. Time taken for the first and second anodization was 10 and 3 minutes, respectively. In the context of fabricating AAO pores with diameter and wall thickness of 200 nm, two-step anodization using oxalic acid and phosphoric acid was attempted. The initial step is to create a template for the oxide growth along with the pore formation. Oxalic acid anodization was carried out at a potential of 40 V, keeping the temperature constant at 280 K.

3.1 *Step one of anodization using oxalic acid*

The arrangement of pores and structural features of the oxide layer formed after anodization with different concentrations of oxalic acid are characterized using FE-SEM images. Pore diameter is the diameter of the circular holes formed on the alumina and wall thickness is the distance between one edge of the pore to the other edge of neighbouring pore. Table 1 shows the variations of pore diameter and wall thickness for increasing

Table 1. Anodization using oxalic acid at a constant time, temperature and voltage of 10 min, 280 K and 40 V respectively.

Sample no.	Weight (%)	Pore diameter (nm)	Wall thickness (nm)
1	3.7821	96	50
2	5.0428	50	75
3	6.3035	45	80

concentration of oxalic acid at constant temperature (280 K) and voltage (40 V). The superlative pore arrangement is perceived at 40 V of anodization voltage when oxalic acid is used as the electrolyte.[28] At anodization potential of 40 V, lower concentration of electrolyte helps in the pore formation with a diameter of 96 nm and wall thickness of 50 nm. An increase in the concentration of the electrolyte is directly proportional to the increase in the wall thickness of porous alumina. In the previous reports, the first anodized samples showed long ordered pore arrangement and high porosity.[29] In this work, less ordered pore arrangement and moderate porous template are fabricated by decreasing the time of anodization. Figure 1 shows the FE-SEM image of sample number-1 from table 1.

It is apparent from figure 1 that the pore formation is coarsely uniform and equally spaced at lower concentrations of oxalic acid. The pore diameter (nm) of the first anodized samples increased linearly with the increase in the concentration of oxalic acid (figure 2). The relation between the pore diameter in nm and oxalic acid concentration is given as,

$$\text{Pore diameter } (D_p) = 14.387 \times -16.529 \qquad (1)$$

where x is concentration of oxalic acid in the range of 2.5-5 wt%. Cell diameter is the dimension of pore diameter including the wall thickness. The cell diameter is constant around 80-120 nm, while the porosity increased from 10% to 30% with the increase in the concentration of oxalic acid. Above 4.4 wt% of oxalic acid, the porosity and pore diameter started decreasing. In this paper, 3.78 wt% concentration of oxalic acid was chosen due to the self-ordered regime behaviour of the aluminium layer. Porosity (P) is calculated using the formula,[30]

$$\mathrm{P} = \left(\frac{\pi}{2\sqrt{3}}\right)\left(\frac{D_p}{D_c}\right)^2 \qquad (2)$$

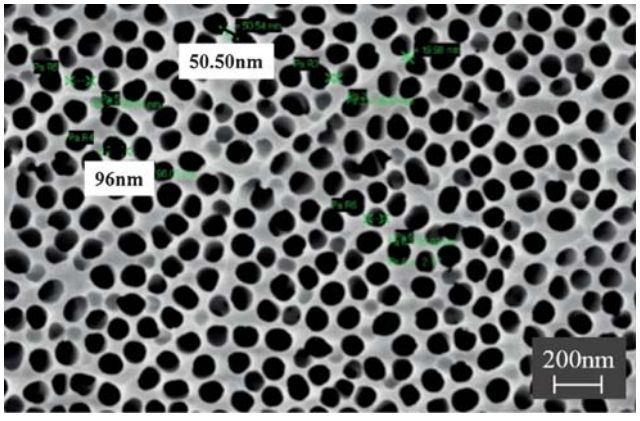

Figure 1. SEM morphological image of sample no.1 from table 1.

D_p and D_c are pore diameter and interpore distance respectively.

After first anodization, the oxide layer was removed using the mixture of H_3PO_4 and H_2CrO_4, leaving behind the weak spots for second anodization.

3.2 *Step two with Orthophosphoric acid*

Anodization carried out with orthophosphoric acid at room temperature resulted in 120 nm pore diameter and 40 nm wall thickness with no-self ordering. This result agrees with the findings of Masuda *et al.,*[3] where the anodization was processed at 150 V. The irregularities were observed because of the heat generated on the surface of the electrolyte due to high anodization voltage. To overcome the irregularities, the experiments were conducted on pre-anodized samples, which resulted in improved pore arrangement and physical properties of the porous alumina. Table 2 shows the variations in pore diameter and wall thickness in relation to the time of anodization. Inter-pore distance and pore diameter of the second anodized samples were calculated from FE-SEM top-view images for different anodization timing.

In the second anodization, the time of anodization was varied from 1 min to 3 min (figure 3). Figure 4 shows the relationship between anodization time and cell or pore diameter along with porosity. Even though the cell and pore diameter increased linearly, the porosity

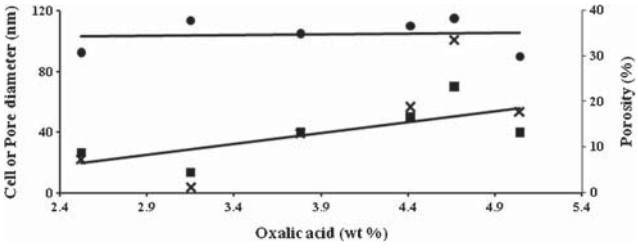

Figure 2. Relationship between concentration of oxalic acid in wt%, cell diameter in nm (●), pore diameter in nm (■) and porosity in % (×).

Table 2. Re-anodization at constant temperature (293 K) and voltage (150 V) by varying the time of anodization.

Sample No.	Time (min)	Pore diameter (nm)	Wall thickness (nm)
1	2.2	130	128
2	2.5	150	100
3	3.1	180	130
4	3.16	200	130

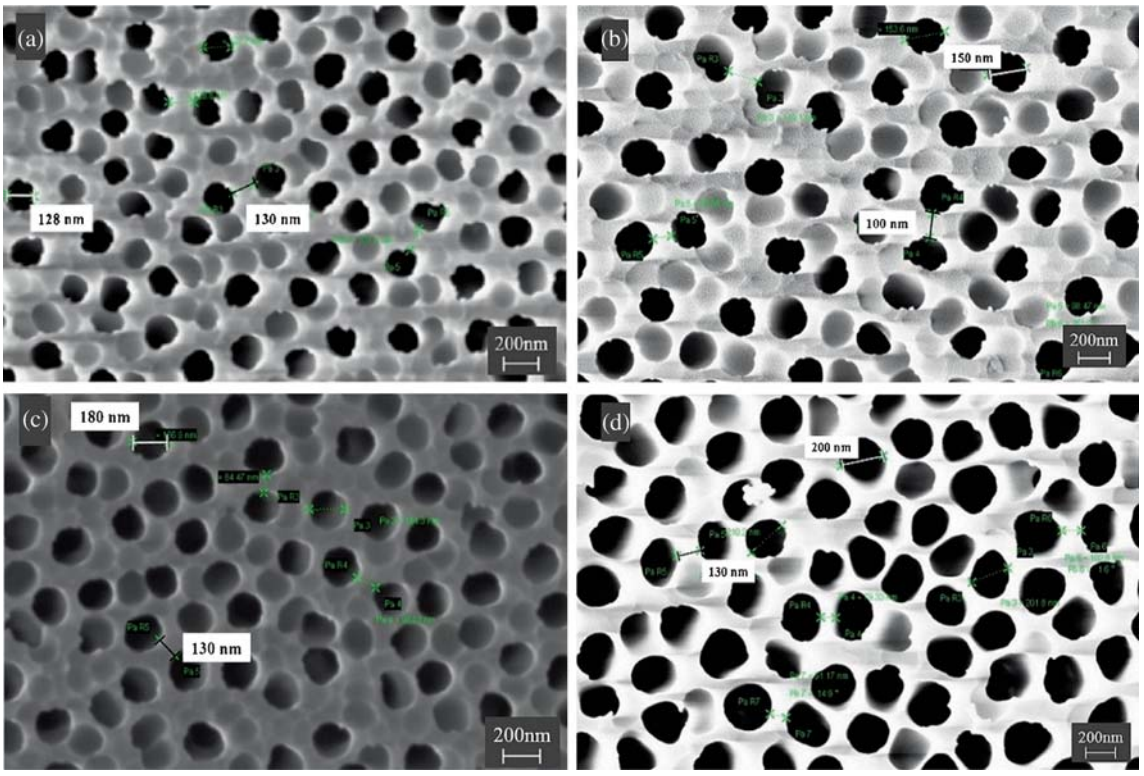

Figure 3. FE-SEM top-view micrographs for various times of re-anodization: 2.2 min (**a**), 2.5 min (**b**), 3.1 min (**c**) and 3.16 min (**d**) carried out in 1% phosphoric acid. The first anodization was carried out in 0.3 M oxalic acid electrolyte at 280 K and 40 V.

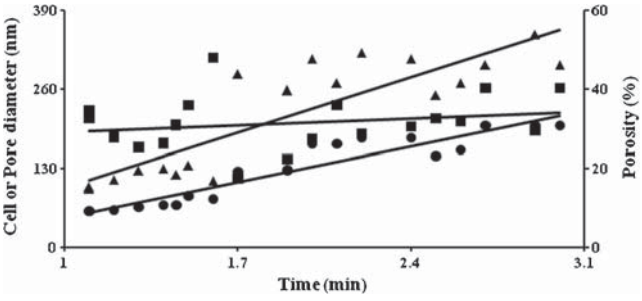

Figure 4. Relationship between anodization time in minutes with cell diameter in nm (▲), pore diameter in nm (●) and porosity in % (■).

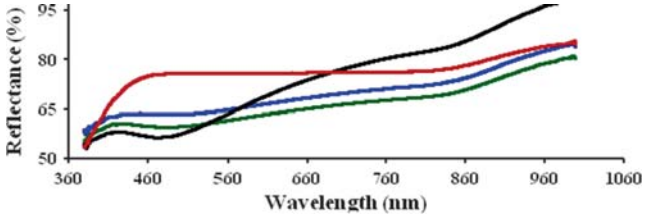

Figure 5. Reflection spectra of the re-anodized porous alumina formed using 1% phosphoric acid for different pore diameter: cell diameter in nm 139:176 (black), 114:153 (green), 84:156 (blue) and 56:67 (red).

is observed to be maximized (47%) at 1.6 min. Above 1.6 min of anodization time, the porosity was verified to be saturated around 30%. The pore diameter obtained increased with increase in time from 130–200 nm. The irregularity of pore arrangement in the first anodization had no effect in the pore formation by second anodization. The current density in second anodization was very small, so the Al^{3+} dissolution is from the bottom of the pores. By increasing the anodization time, the height of the oxide layer was increased and the regularity of long pore channel was not affected.[31]

3.3 *Reflectance of anodized aluminium*

Reflection spectra of re-anodized porous alumina of different pore size (d) and wall thickness (t) are shown in figure 5. According to the previous reports, the transmittance increases as the anodised membrane is heated to 973 K.[32] From figure 5, it can be identified that when the pore diameter is 56 nm the reflectance average is 76% and as the pore diameter increases to 84, 114 and 139 nm, the reflectance averages are 69, 66, and 74%, respectively. In the sample with pore diameter 139 nm and wall thickness 176 nm, the reflectance is high (80%) at wavelength 730 nm and it drops down to 56% at 480 nm. There is a noticeable difference in

the absorption of the solar spectrum as the porosity increases. The surface area of the alumina substrate also increases along with the increase in the porosity, making a way for further interaction between the photons in the solar spectrum and the Al_2O_3 which leads to higher absorption factor due to total internal reflection.

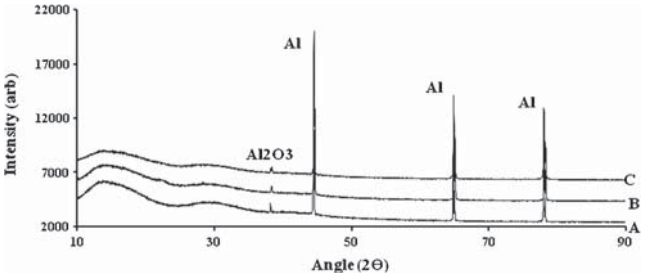

Figure 6. XRD pattern of (A) aluminum, (B) first anodized alumina and (C) second anodized alumina.

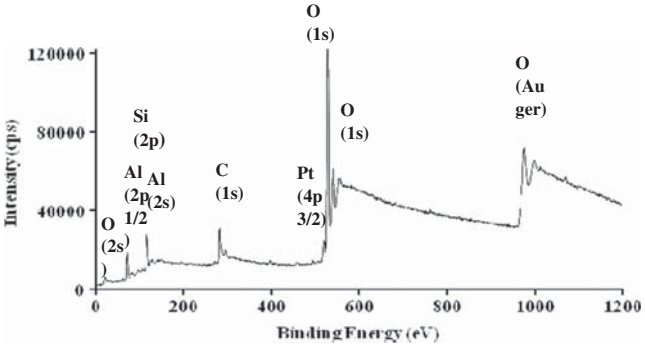

Figure 7. X-ray photoelectron spectrum of two-step anodized alumina after the oxide growth for 3 min in phosphoric acid.

3.4 *X-Ray diffraction (XRD) analysis*

Figure 6 shows the X-ray diffraction pattern of aluminium and anodized aluminium samples. From the diffraction pattern, it is noticed that the Al and Al_2O_3 phases are present in the anodized sample. This infers that after anodization, the porous Al_2O_3 layer was formed on the substrate. X'pert high score plus (version 2.0) is used to identify the peaks. In figure 6A, the aluminium peaks that appeared at $2\theta = 44.48$, 64.88 and 78.03 (JCPDS file no. 01-089-2837) confirmed the cubic structure of Al substrate. After first anodization, the tetragonal Al_2O_3 peaks were observed at $2\theta = 38.29$ (JCPDS file no. 04-016-7505) as shown in figure 6B. The peaks of the re-anodized sample which occurred at $2\theta = 38.32$ (JCPDS file no. 04-016-7505) indicates the tetragonal structure of Al_2O_3 as shown in figure 6C.

3.5 *X-ray photo electron spectroscopic (XPS) analysis*

XPS spectra of the re-anodized aluminium oxide layer are shown in figure 7. The intensity peaks of the anodized aluminium correspond with the general spectra of Al_2O_3.[33] The impurity peaks identified with Platinium (Pt) and Silicon (Si) originated from the electrode and the substrate used when anodization was carried out. The sample showed traces of Pt and Si on the surface, apart from aluminium (Al), oxygen (O) and carbon (C). Figure 8a shows the high-resolution Al 2p spectra of the re-anodized aluminium sample. The binding energy of the Al 2p is located at 73.1 eV which matches the orbital value of Al $2p_{3/2}$, for O 1s at 530.9 eV and C 1s at 283.6 eV as shown in figure 8a, b and c, respectively. From this analysis, it is verified that the AAO film

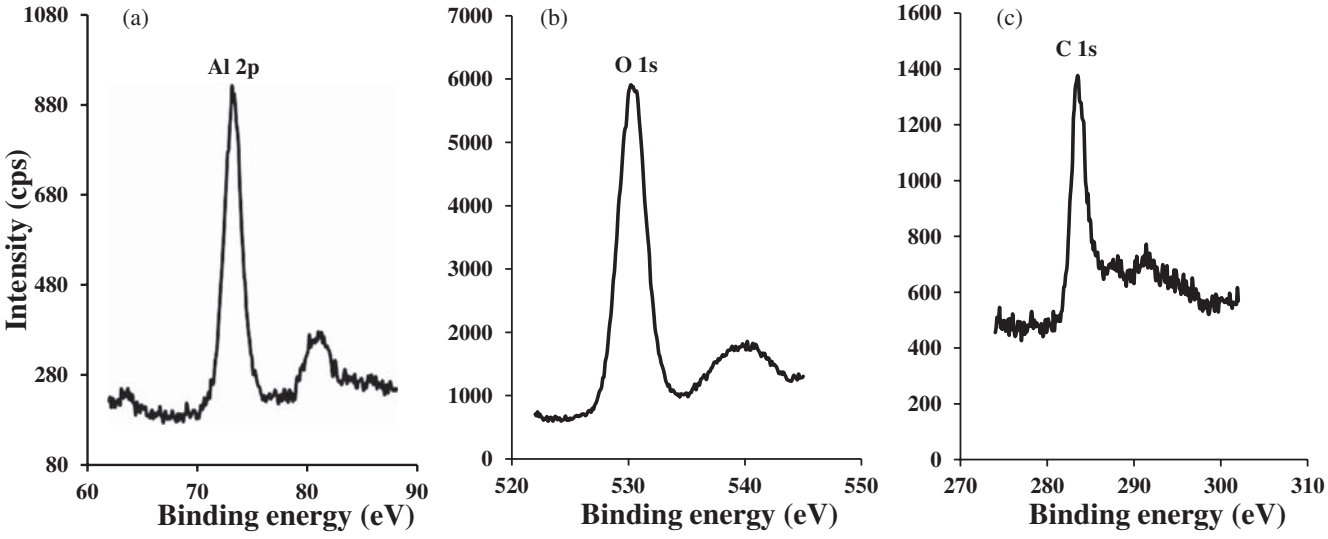

Figure 8. X-ray photoelectron spectra of two-step anodized alumina after the growth of oxide layer: Al 2p (**a**), O 1s (**b**) and C 1s (**c**).

fabricated by two-step anodization does not contain any alloying elements.

4. Conclusions

A fast anodization process that takes less than 15 min is described. It is a two-step anodization process and the pore formation was found to be dependent on the temperature of the electrolyte. Varying the time of anodization process, the pore density can be controlled. Based on the two-step anodization process, oval-shaped pores were formed with 180 nm pore diameter and 130 nm wall thickness. The ratio of light absorption by anodized samples with different pore sizes increased with an increase in surface area. Therefore, while using anodized alumina in thin-film solar cells, it is anticipated to be beneficial for enhanced light trapping. XRD analysis showed the existence of Al_2O_3 peaks after anodization. And XPS data of anodized Al showed traces of Al, O, C, Si and Pt along with their orbital values. The presented method of ultra-fast anodization can be tuned for further control over the pore size and its arrangement.

References

1. Routkevitch D, Bigioni T, Martin M and Jing M X 1996 *J. Phys. Chem.* **100** 14037
2. O'Sullivan J P and Wood G C 1970 *Proc. Roy. Soc. Lond. A* **317** 511
3. Masuda H and Fukuda K 1995 *Science* **268** 1466
4. Diggle J W, Thomas C D and Goulding C W 1969 *Chem. Rev.* **69** 365
5. Nielsch K, Choi J, Schwirn K, Wehrspohn R B and Gösele U 2002 *Nano Lett.* **2** 677
6. Ono S, Saito M and Asoh H 2005 *Electrochem. Micro Nano Tech.* **51** 827
7. Kikuchi T, Yamamoto T and Suzuki R O 2013 *Appl. Surf. Sci.* **284** 907
8. Sulka G D and Stepniowski W J 2009 *Electrochim. Acta* **54** 3683
9. Lu C and Zhi C 2011 *Encyclopedia of Nanoscience and Nanotechnology* **11** 235
10. Poinern G E J P, Ali N and Fawcett D 2011 *Materials* **4** 487
11. Ono S and Masuko N 2003 *Surf. Coat. Tech.* **169-170** 139
12. Sulka G D, Stroobants S, Moshchalkov V, Borghs G and Celis J P 2002 *J. Electrochem. Soc.* **149D** 97
13. Buijnsters J G, Rui Z, Natalia T and Celis J P 2013 *ACS Appl. Mater. Interfaces* **5** 3224
14. Coz F L, Arurault L and Datas L 2010 *Mater. Charact.* **61** 283
15. Nguyen T N, Kim D, Jeong D-Y, Kim M-W and Uk Kim J 2012 *Electrochim. Acta* **83** 288
16. Masuda H, Yamada H, Satoh M, Asoh H, Nakao M and Tamamura T 1997 *Appl. Phys. Lett.* **71** 2770
17. Jessensky O, Müller F and Gösele U 1998 *J. Electrochem. Soc.* **145** 3735
18. Chung C K, Liao M W, Chang H C and Lee C T 2011 *Thin Solid Films* **520** 1554
19. Sulka G D, Stroobants S, Moshchalkov V V, Borghs G and Celis J P 2004 *J. Electrochem. Soc.* **151B** 260
20. Lee W, Ji R, Gösele U and Nielsch K 2006 *Nature Mater.* **5** 741
21. Ono S, Saito M and Asoh H 2005 *Electrochim. Acta* **51** 827
22. Debuyck F, Moors M and Peteghem A P V 1993 *Mater. Chem. Phys.* **36** 146
23. Li A P, Müller F, Birner A, Nielsch K and Gösele U 1998 *J. Appl. Phys.* **84** 6023
24. Bae E J, Choi W B, Jeong K S, Chu J U, Park G S, Song S and Yoo I K 2002 *Adv. Mater.* **14** 277
25. Liu J, Liu S, Zhou H, Xie C, Huang Z, Fu C and Kuang Y 2014 *Thin Solid Films* **552** 75
26. Sulka G D and Stępniowski W J 2009 *Electrochim. Acta* **54** 3683
27. Sousa C T, Leitao D C, Proenca M P, Ventura J, Pereira A M and Araujo J P 2014 *Appl. Phys. Rev.* **1** 031102
28. Vrublevsky I A, Chernyakova K V, Ispas A, Bund A and Zavadski S 2014 *Thin Solid Films* **556** 230
29. Crist B V 1999 In *Handbooks of Monochromatic XPS Spectra* **2** (California: XPS International LLC)
30. Surawathanawises K and Cheng X 2014 *Electrochim. Acta* **117** 498
31. Li F, Zhang L and Metzger R M 1998 *Chem. Mater.* **10** 2470
32. Zaraska L, Stepniowski W J, Sulka G D, Ciepiela E and Jaskuła M 2013 *Appl. Phys. A* **114** 571
33. Li Y, Zheng M, Ma L and Shen W 2006 *Nanotechnology* **17** 5101